Cell. Mol. Life Sci. (2015) 72:3185–3200
DOI 10.1007/s00018-015-1890-6

Cellular and Molecular Life Sciences

RESEARCH ARTICLE

F-actin binding protein, anillin, regulates integrity of intercellular junctions in human epithelial cells

Dongdong Wang[1] · Gibran K. Chadha[1] · Alex Feygin[1] · Andrei I. Ivanov[1,2,3]

Received: 15 September 2014 / Revised: 26 February 2015 / Accepted: 19 March 2015 / Published online: 27 March 2015

Abstract Tight junctions (TJ) and adherens junctions (AJ) are key morphological features of differentiated epithelial cells that regulate the integrity and permeability of tissue barriers. Structure and remodeling of epithelial junctions depends on their association with the underlying actomyosin cytoskeleton. Anillin is a unique scaffolding protein interacting with different cytoskeletal components, including actin filaments and myosin motors. Its role in the regulation of mammalian epithelial junctions remains unexplored. Downregulation of anillin expression in human prostate, colonic, and lung epithelial cells triggered AJ and TJ disassembly without altering the expression of junctional proteins. This junctional disassembly was accompanied by dramatic disorganization of the perijunctional actomyosin belt; while the general architecture of the actin cytoskeleton, and activation status of non-muscle myosin II, remained unchanged. Furthermore, loss of anillin disrupted the adducin–spectrin membrane skeleton at the areas of cell–cell contact, selectively decreased γ-adducin expression, and induced cytoplasmic aggregation of αII-spectrin. Anillin knockdown activated c-Jun N-terminal kinase (JNK), and JNK inhibition restored AJ and TJ integrity and cytoskeletal organization in anillin-depleted cells. These findings suggest a novel role for anillin in regulating intercellular adhesion in model human epithelia by mechanisms involving the suppression of JNK activity and controlling the assembly of the perijunctional cytoskeleton.

Keywords Tight junctions · Adherens junctions · Non-muscle myosin II · Adducin · Spectrin · JNK

D. Wang and G. K. Chadha contributed equally to the paper.

Electronic supplementary material The online version of this article (doi:10.1007/s00018-015-1890-6) contains supplementary material, which is available to authorized users.

✉ Andrei I. Ivanov
aivanov2@vcu.edu

[1] Department of Human and Molecular Genetics, Virginia Commonwealth University, 401 College Street, Box 980035, Richmond, VA 23298, USA

[2] Virginia Institute of Molecular Medicine, Virginia Commonwealth University, Richmond, VA 23298, USA

[3] VCU Massey Cancer Center, Virginia Commonwealth University, Richmond, VA 23298, USA

Introduction

Among the most important functions of epithelial cells is the formation of tissue barriers that protect internal organs from the noxious environment, along with generating their unique architecture and chemical composition [1–3]. The integrity and barrier properties of epithelial layers are regulated by intercellular junctions that represent multiprotein complexes assembled at the plasma membrane of contacting cells [4, 5]. Well-differentiated epithelial cells form several types of junctions; among them, adherens junctions (AJ) and tight junctions (TJ) are the major determinants of epithelial integrity and permeability [1, 6–10]. The structure and functions of AJ and TJ are regulated by different mechanisms, including cytoskeletal rearrangements and vesicle trafficking [2, 11–15]. The actin cytoskeleton is known to be especially important in preserving the integrity and mediating the remodeling of epithelial junctions. Indeed, one of the most characteristic F-actin structures of polarized epithelial cells is a circumferential belt that is closely associated with AJ [16, 17]. Likewise, TJ appear to be connected with an elaborate

network of apical F-actin bundles [18]. The actin cytoskeleton plays several major functions at epithelial junctions [12, 19–21]. It clusters and stabilizes nascent adhesive contacts, thereby mediating their transformation into large multiprotein ensembles. It also limits intramembrane mobility of junctional proteins and prevents their endocytosis from the plasma membrane. This activity increases the strength of intercellular adhesions and tightens the epithelial barrier. Furthermore, junction-associated F-actin senses and transduces mechanical forces, thus orchestrating responses of multiple cells within the epithelial layer. This feature is critical for epithelial morphogenesis and wound healing. Finally, F-actin remodeling serves as a driver of junctional disassembly and reassembly, thereby mediating epithelial plasticity. The actin cytoskeleton is the subject of complex regulation involving a large number of structural, scaffolding, and signaling molecules [22, 23]. They include proteins that drive actin filament turnover, myosin motors, small GTPases, kinases, and phosphatases. Many of these proteins are known to affect AJ/TJ structure and permeability by controlling the assembly and the dynamics of junction-associated actin filaments [19, 24–26].

Anillin is a multifunctional scaffolding protein that regulates different cytoskeletal structures during specific stages of the cell cycle [27–29]. Anillin directly binds to actin filaments and induces filament bundling [30, 31]. It also interacts with non-muscle myosin (NM) II and controls localization and activity of NM II in contractile rings [32–34]. Finally, anillin is capable of activating Rho A and recruiting this small GTPase to actomyosin bundles [33, 35]. Anillin plays a prominent role in cytokinesis by regulating cleavage furrow positioning and ingression during the separation of a dividing cell into daughter cells [27–29]. It is also involved in the transformation of the cellular cortex during early developmental events such as cellularization and polar body emission [30, 32, 36]. However, little is known about anillin's function outside cell division. Interestingly, recent reports have implicated this scaffolding protein in the regulation of extracellular matrix adhesion and intercellular junctions. Thus, a missense point mutation of anillin was identified as a cause of a genetic kidney disorder, focal segmental glomerulosclerosis, which is characterized by defects in podosomal matrix adhesions [37]. Furthermore, a genome-wide genetic screen identified anillin as one of the regulators of cadherin-mediated cell–cell adhesion in *Drosophila* [38]. Finally, knockdown of anillin resulted in abnormal AJ and TJ structure in *Xenopus* embryos [39]. However, it remains unknown whether or not anillin is essential for the stability and remodeling of intercellular contacts in mammalian tissues. The present study was designed to address this question, by investigating the roles of anillin in regulating AJ and TJ structure in model human epithelial monolayers.

Materials and methods

Antibodies and other reagents

The following primary monoclonal (mAb) and polyclonal (pAb) antibodies were used to detect cytoskeletal, junctional, and signaling proteins: anti-anillin (A301-405A and A301-406A) and MgcRacGAP pAbs (Bethyl Laboratories, Montgomery, TX); anti-anillin pAb (Bioss, Woburn, MA); anti-p120-catenin, E-cadherin, αII-spectrin, and βII-spectrin mAbs (BD Biosciences; San Jose, CA); anti-NM IIA, NM IIB, and NM IIC pAbs (Covance; Princeton, NJ); anti-total regulatory myosin light chain (RMLC), monophosphorylated (p), diphosphorylated (pp) RMLC, JNK, p-JNK, ERK1/2, p-ERK1/2, p38 and p-p38 Abs (Cell Signaling Technology; Danvers, MA); anti-ZO-1 and JAM-A pAbs (Invitrogen; Carslbad, CA); anti-cadherin-6 and anti-total actin (clone C4) mAbs (EMD Millipore; Billerica, MA); anti-β-catenin pAb, anti-vinculin, α-tubulin and acetyl-tubulin mAbs (Sigma-Aldrich; St. Louis, MO); anti-α-catenin mAb (Abcam; Cambridge, MA); anti-α-adducin, p-adducin, CD2AP and Ect2 pAbs, and anti-γ-adducin mAb (E-1) (Santa Cruz; Dallas, TX). Anti-JAM-A monoclonal antibody was previously described [40]. Alexa Fluor-488-conjugated donkey anti-rabbit and Alexa Fluor-555-conjugated donkey anti-mouse secondary antibodies and Alexa Fluor-488 and 555-labeled phalloidin were obtained from Invitrogen. Horseradish peroxidase-conjugated goat anti-rabbit and anti-mouse secondary antibodies were acquired from Bio-Rad Laboratories. Y-27632 and SP600125 were purchased from EMD Millipore. All other chemicals were obtained from Sigma-Aldrich.

Cell culture

DU145 human prostate epithelial cells and A549 human lung epithelial cells were acquired from American Type Culture Collection (Manassas, VA). SK-CO15 human colonic epithelial cells were provided by Dr. Enrique Rodriguez-Boulan (Cornell University). DU145 cells were cultured in RPMI medium supplemented with 10 % fetal bovine serum, 15 % HEPES, pyruvate, and antibiotics. A549 and SK-CO15 cells were cultured in DMEM/F12 and DMEM medium, respectively, supplemented with 10 % fetal bovine serum and antibiotics. The cells were grown in T75 flasks (BD Biosciences), and were seeded on collagen-coated coverslips or 6-well plastic plates for immunolabeling and biochemical experiments, respectively.

RNA interference and plasmid expression

Downregulation of anillin expression was carried out using individual small-interfering (si)RNA duplexes 1 (GGAGA UGGAUCAAGCAUUA) and 3 (GGAUAAAUCUGGCU AAUUG) obtained from Dharmacon (Lafayette, CO) or Stealth siRNA duplexes 93 (HSS122893) and 97 (HSS182497) obtained from Invitrogen. Dharmacon non-targeting siRNA duplex 2 and Invitrogen non-coding low GC content duplex 1 were used as appropriate controls. Knockdown of γ-adducin was achieved using siRNA SmartPool (Dharmacon). Cells were transfected using DharmaFect 1 transfection reagent (Dharmacon) with a final siRNA concentration of 50 nM, as described previously [41, 42]. For knockdown/overexpression experiments, DU145 cells plated on coverslips were transfected with either control or anillin-specific siRNAs and 24 h later, were subjected to a second round of transfection with either GFP-γ-adducin plasmid (gift from Dr. Y. Peng Loh, Eunice Kennedy Shriver National Institute of Child Health, Bethesda, MD [43]), or a control GFP plasmid (gift from Dr. Andrei Budanov, VCU, Richmond, VA). The plasmid transfection was carried out using a TransIT-Prostate transfection kit (Mirus Bio, Madison, WI) according to the manufacturer's instructions. The cells were examined 3 days after the second transfection.

Immunoblotting

Cells were homogenized in RIPA lysis buffer (20 mM Tris, 50 mM NaCl, 2 mM EDTA, 2 mM EGTA, 1 % sodium deoxycholate, 1 % Triton X-100 and 0.1 % SDS; pH 7.4), containing protease inhibitor cocktail (1:100; Sigma), phosphatase inhibitor cocktails 2 and 3 (each at 1:200; Sigma-Aldrich), and Pefabloc SC (Roche Diagnostics; Mannheim, Germany). Lysates were cleared by centrifugation (14,000*g* for 20 min), diluted twofold with 2× SDS Laemmli buffer, and boiled for 6 min. SDS-polyacrylamide gel electrophoresis was conducted using standard protocols with an equal amount of total protein per lane (10–20 μg), followed by immunoblotting on nitrocellulose membrane. Protein expression was quantified via densitometry using ImageJ software (National Institute of Health, Bethesda MD). Data are presented as normalized values using expression values in control siRNA-treated groups defined as 100 %.

Quantitative RT-PCR

Total RNA was isolated using the RNeasy mini kit (QIAGEN, Valencia CA) followed by DNase treatment to remove genomic DNA. Total RNA (1 μg) was reverse transcribed using the iScript cDNA synthesis kit (Bio-Rad Laboratories, Hercules, CA). Quantitative real-time PCR was performed using iTaq Universal SYBR Green Supermix (Bio-Rad Laboratories) and 7900HT Fast Real-time PCR System (Applied Biosystems; Foster City, CA). The following primers were used: human-glyceraldehyde 3-phosphate dehydrogenase (GAPDH) (NM_002046.5), forward-CATGTTCGTCATGGGTGTGAACCA, reverse-AGTGATGGCATGGACTGTGGTCAT; α-adducin (NM_176801.1), forward-TCTGGGCTACAGAACTGGCT, reverse-TCTTCGACTTGGGACTGCTT; β-adducin (NM_017484.2), forward-TTCCCCTGTGATCTTGGGTGCCG GT, reverse-AGTGCCCACAGGGGCCATCAGACAT; γ-adducin (NM_016824.3), forward-CACCTCCTCTCAG TCTTGGC, reverse-GCTGTTGCAAGGGTATGGAT. Primers were designed to amplify all known transcript variants of adducin isoforms. GAPDH was quantified as a stably expressed reference gene. Expression of adducins was normalized to GAPDH, which served as an internal control for calibrating the quantity of RNA isolated from each sample. Threshold cycle number for the gene of interest (Ct) was calculated based on the amplification curve representing a plot of the fluorescent signal intensity versus the cycle number. The relative expression of each gene was calculated using the comparative Ct method with the formula $2^{-\Delta\Delta Ct}$ (where $\Delta Ct = Ct_{adducin} - Ct_{GAPDH}$ and $\Delta\Delta Ct = \Delta Ct$ of anillin siRNA-transfected cells $- \Delta Ct$ of control siRNA-transfected cells).

Immunofluorescence labeling and confocal microscopy

DU145, A549, and SK-CO15 cell monolayers plated on collagen-coated coverslips were fixed in 100 % methanol for 20 min at −20 °C. In order to visualize anillin, GFP-γ-adducin, and the actin cytoskeleton, cells were fixed with 4 % PFA and permeabilized with 0.5 % Triton X-100 at room temperature. Fixed cells were blocked for 60 min at room temperature in HEPES-buffered Hanks balanced salt solution containing 1 % bovine serum albumin. After blocking, cells were incubated with the appropriate concentrations of primary antibodies in blocking solution for 60 min. Cells were then washed and incubated with Alexa dye-conjugated secondary antibodies for 60 min, rinsed with blocking buffer, and mounted on slides with ProLong Antifade mounting reagent (Invitrogen). Labeled cell monolayers were observed using a Zeiss LSM 700 Laser Scanning Confocal Microscope (Carl Zeiss Microimaging Inc.; Thornwood; NY). The Alexa Fluor 488 and 555 signals were imaged sequentially in frame-interlace mode to eliminate cross-talk between channels. Image analysis was conducted using imaging software ZEN 2011 (Carl Zeiss Microscopy Inc.) and Adobe Photoshop. Images shown are representative

of at least 3 experiments. Multiple images were captured from each slide.

Cell dissociation and permeability assays

DU145 cells seeded on 6-well plates were transfected with either control or anillin-specific siRNAs. On day 4 post-transfection, the cells were washed with PBS, scraped away from the plastic, and mechanically dissociated by pipetting 30 times as previously described [44]. The number of cell clusters (particles; Np) containing more than three cells was counted under a microscope with a hemocytometer. Afterwards, the cell particles were pelleted by centrifugation and resuspended in 0.05 % trypsin/EDTA solution to disrupt all cell aggregates. Trypsinized cells were pelleted, resuspended in cell culture medium, and counted to obtain the total cell number (Nc). The cell dissociation index was calculated and expressed as Np/Nc $\times$ 100 %.

Transepithelial electrical resistance (TEER) of SK-CO15 cell monolayers was measured using an EVOMX voltohmmeter (World Precision Instruments, Sarasota, FL). The resistance of cell-free collagen-coated filters was subtracted from each experimental point.

Statistics

All numerical values from individual experiments were pooled and expressed as mean $\pm$ standard error of the mean (SE) throughout. Obtained numbers were compared by two-tailed Student's t test, with statistical significance assumed at $p < 0.05$.

Results

Downregulation of anillin expression resulted in disassembly of epithelial junctions

In order to examine the roles of anillin in the regulation of epithelial junctions, we used RNA interference to down-regulate its expression in DU145 prostate epithelial cells. Two different siRNA duplexes decreased anillin protein levels by 99 % on day 4 post-transfection (Fig. 1a). These knockdowns significantly weakened epithelial cell–cell adhesions, as indicated by their decreased resistance to mechanic stress in the cell dissociation assay (Fig. 1b). Immunolabeling and confocal microscopy revealed dramatic morphological changes of anillin-depleted DU145 cells characterized by a significant increase in cell size (Fig. 1c) and multinucleation (data not shown). The observed phenotype is consistent with previous reports of large multinuclear anillin-deficient cells in vitro and in model organisms [32, 35, 45] and reflects defective cytokinesis. Furthermore, loss of anillin resulted in marked TJ and AJ disassembly on days 3 and 4 post-siRNA-transfection. Thus, control DU145 cell monolayers were characterized by a continuous linear labeling of TJ proteins, ZO-1, JAM-A, and occludin at the areas of cell contact (Fig. 1c, arrows). This pattern was transformed into a discontinuous, bead-like labeling pattern in anillin-depleted cells, indicating a breakdown of TJ integrity (Fig. 1c, arrowheads). Furthermore, anillin knockdown distorted localization of AJ proteins, E-cadherin, cadherin-6, and β-catenin, at intercellular contacts, and caused these proteins to redistribute into cytoplasmic vesicles (Fig. 2, arrowheads). Such alterations of AJ and TJ structure were reproducibly observed in DU145 cells transfected with four different siRNA duplexes obtained from two different commercial sources (Dharmacon and Invitrogen). Importantly, anillin knockdown also triggered AJ/TJ disassembly in A549 lung epithelial cells and SK-CO15 colonic epithelial cells (Suppl. Fig. 1a, arrowheads), and decreased TEER values in SK-CO15 cell monolayers; indicating a breakdown of the paracellular barrier (Suppl. Fig. 1b).

Next we sought to elucidate mechanisms that mediate disruption of epithelial junctions in anillin-depleted cells by examining the expression of different junctional proteins. However, immunoblotting analysis did not reveal significant effects of anillin knockdown on the levels of key molecular constituents of AJ and TJ (Suppl. Fig. 2). We also asked if anillin itself is a component of epithelial junctions. In confluent DU145 (Fig. 3, arrows), SK-CO15 (Suppl. Fig. 3), and A549 (data not shown) cell monolayers, anillin was predominantly localized in the nucleus and did not accumulate at intercellular junctions. We tested three different anti-anillin polyclonal antibodies that consistently demonstrated either nuclear or more diffuse nuclear/cytoplasmic labeling of this protein without significant localization at epithelial junctions (data not shown). Furthermore, siRNA-mediated depletion of anillin resulted in the disappearance of its nuclear signal (Fig. 3), thereby validating specificity of the antibody labeling. Together this data suggests that anillin is essential for the assembly of human epithelial junctions and that it likely acts indirectly, without being enriched at the junctional complexes.

Loss of anillin disrupted the perijunctional actomyosin cytoskeleton

Since anillin is a versatile scaffolding protein interacting with different cytoskeletal structures such as actin filaments, myofibrils, and microtubules, its effects on epithelial junctions may be mediated by the cytoskeleton. To test this hypothesis, we examined the effects of anillin depletion on the architecture of filamentous (F) actin and

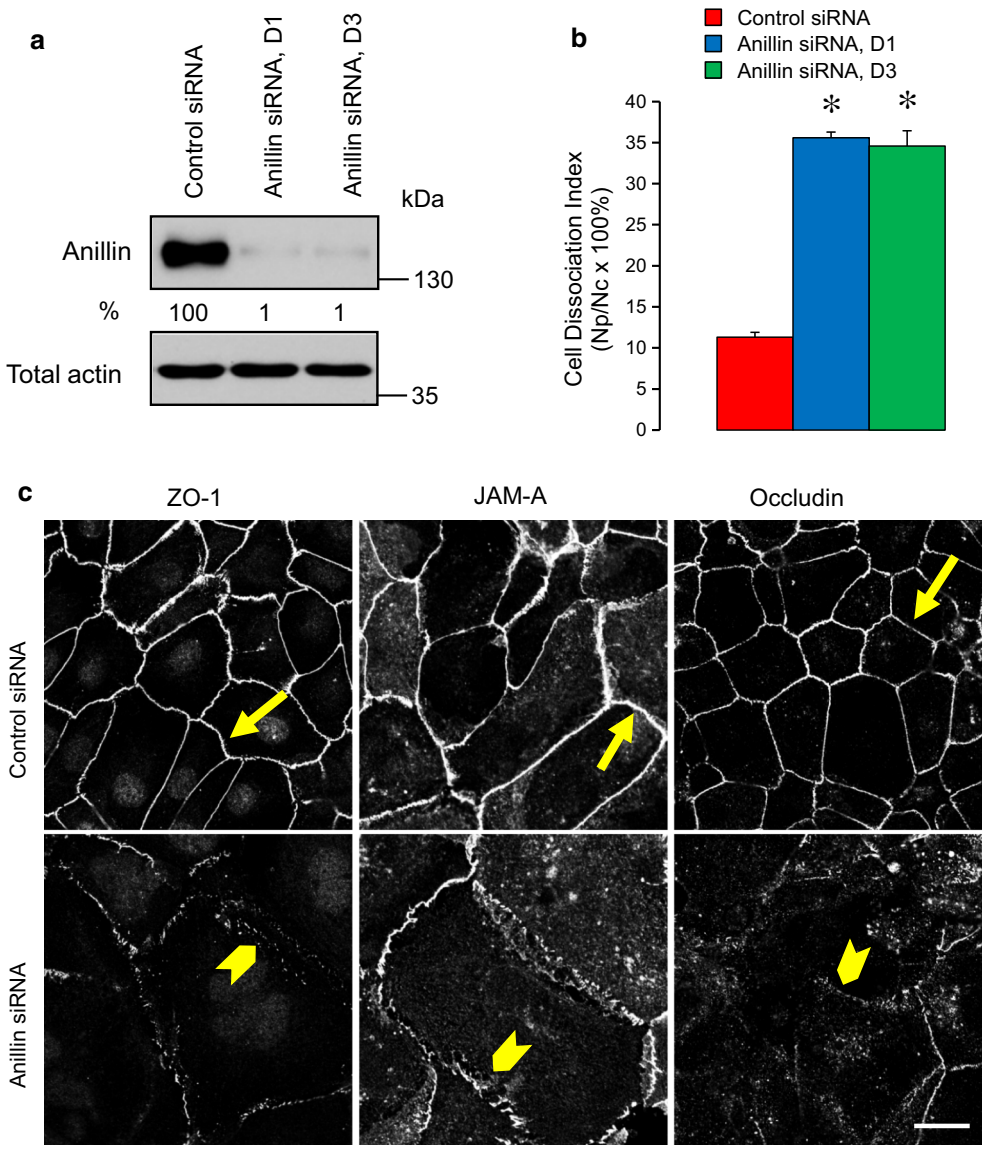

Fig. 1 Anillin depletion weakens intercellular contacts and induces tight junction disassembly in prostate epithelial cells. DU145 cells were transfected with either control or two anillin-specific siRNA duplexes (D1 and D3) and examined on day 4 post-transfection. **a** Efficiency of anillin knockdown was determined by immunoblotting with quantitative densitometric analysis. **b** Avidity of intercellular contact was determined by cell dissociation assay. **c** Morphology of tight junctions was examined using immunofluorescent labeling of ZO-1, JAM-A, and occludin. *Arrows* indicate normal tight junction structure in control siRNA-transfected cells. *Arrowheads* highlight areas of tight junction disassembly in anillin-depleted cells. Data are presented as mean ± SE ($n = 3$); *$p < 0.001$. *Scale bar* 20 μm

microtubules. Control DU145 cell monolayers demonstrated a prominent circumferential F-actin belt associated with epithelial junctions (Fig. 4a, arrows). This F-actin belt disappeared in anillin-depleted cells, where cortical actin filaments were organized into loosely packed bundles positioned in parallel to areas of cell–cell contact (Fig. 4a, arrowheads). Unlike the actin cytoskeleton, microtubule organization and stability was unaffected by anillin depletion, as indicated by immunolabeling of either total, or stable, acetylated microtubules (Suppl. Fig. 4).

Given the key role of NM II in controlling the integrity of the circumferential F-actin belt [12, 26], and the known anillin-dependent regulation of NM II function during cytokinesis [32–34], we next analyzed the effects of anillin depletion on organization and activation of NM II. In control DU145 cells, NM II motor was associated with the perijunctional F-actin belt (Fig. 4b, arrows). Remarkably, junctional localization of NM II was lost in anillin-depleted cell monolayers, where this motor predominantly localized at the basal stress fibers (Fig. 4b, arrowheads). According to immunoblotting analysis, downregulation of anillin did not

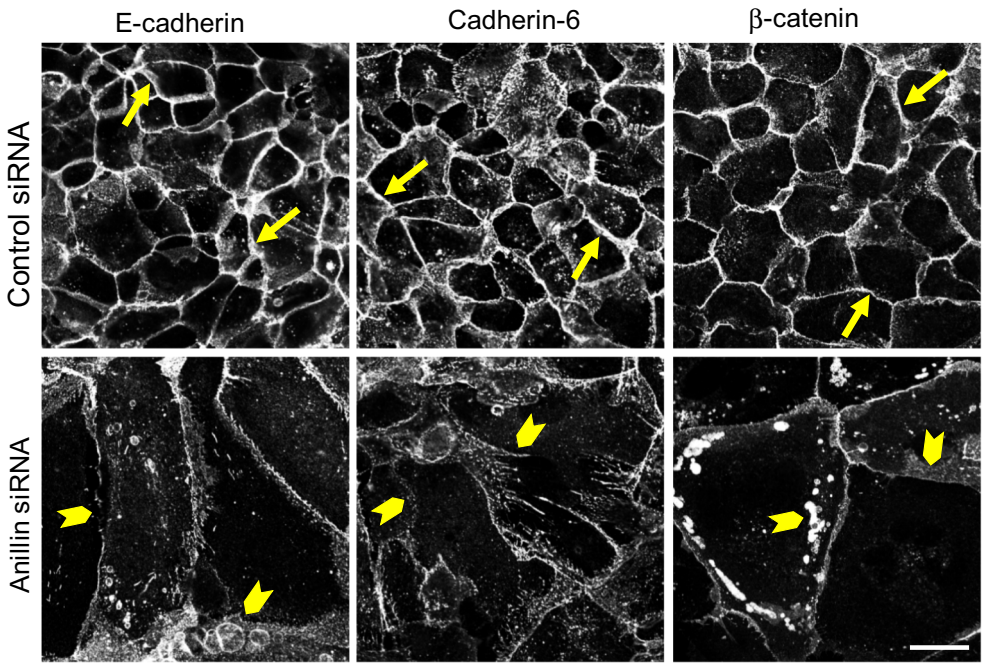

Fig. 2 Anillin depletion disrupts the integrity of epithelial adherens junctions. DU145 cells were transfected with either control or anillin-specific siRNAs and immunolabeled for adherens junction proteins E-cadherin, Cadherin 6, and β-catenin on day 4 post-transfection. *Arrows* indicate accumulation of all adherens junction proteins at the areas of cell–cell contact in control cells. *Arrowheads* highlight the disappearance of these proteins from intercellular junctions after anillin depletion. *Scale bar* 20 μm

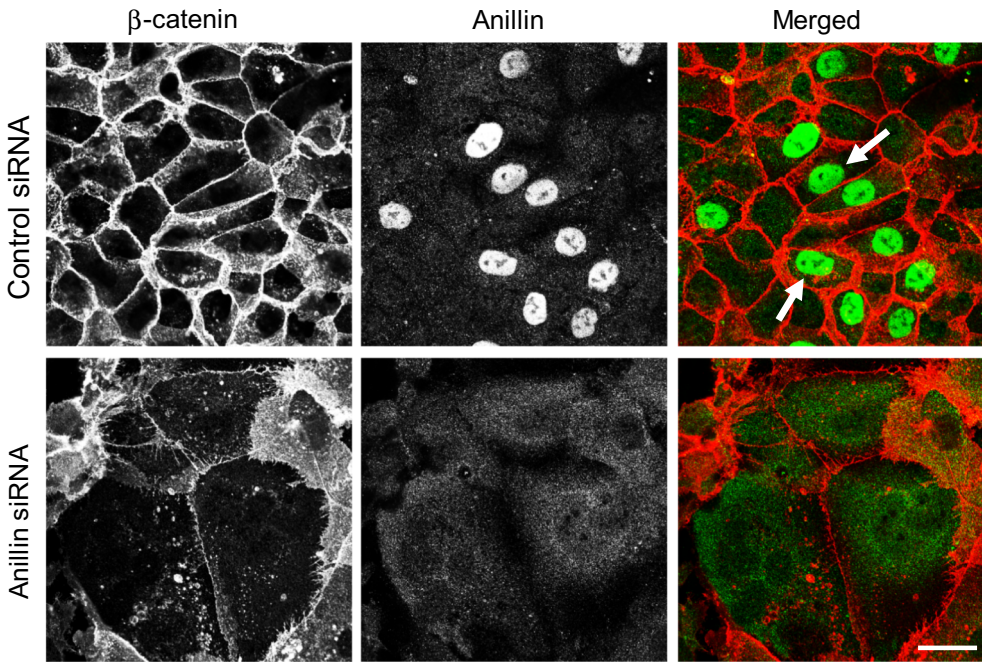

Fig. 3 Anillin does not localize at intercellular junctions in confluent epithelial cell monolayers. Control and anillin-depleted DU145 cell monolayers were subjected to dual immunolabeling for anillin (*green*) and β-catenin (*red*). *Arrows* indicate specific nuclear localization of anillin in control DU145 cells. This nuclear labeling disappears after siRNA-mediated anillin depletion. *Scale bar* 20 μm

alter the expression of myosin heavy chain isoforms, NM IIA, IIB, and IIC (Fig. 5a, b). Furthermore, the overall activation status of NM II was not affected as indicated by unaltered levels of either monophosphorylated of diphosphorylated regulatory myosin light chain (RMLC, Fig. 5a, b). Interestingly, phosphorylated RMLC was enriched at intercellular junctions of control, but not anillin-depleted DU145 cells (Fig. 5c). These results suggest that local dephosphorylation of RMLC at intercellular junctions could inactivate NM II, thereby triggering disintegration of the perijunctional acto-myosin bundles and AJ/TJ disassembly. We tested this hypothesis by blocking RMLC phosphorylation with a

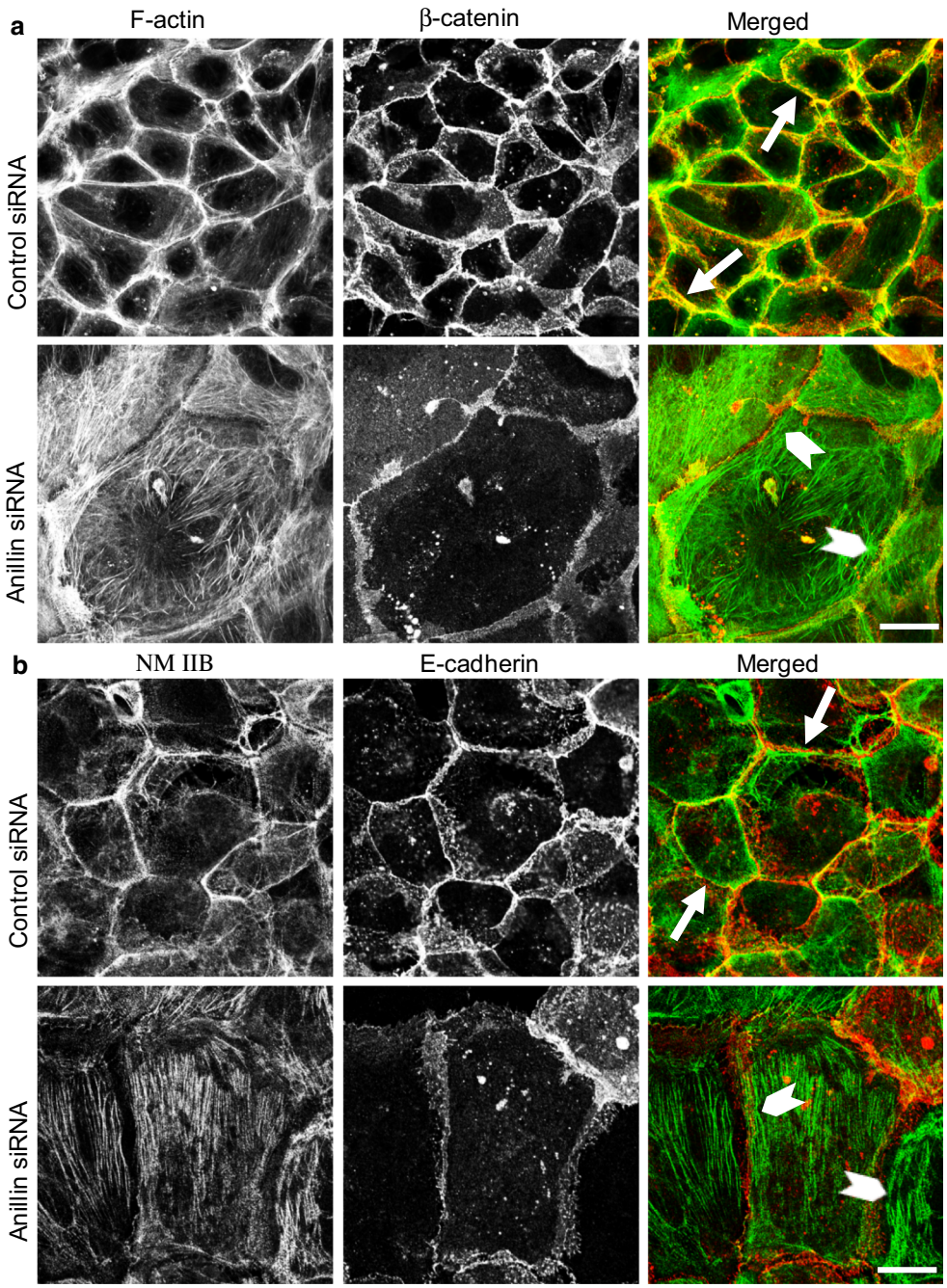

Fig. 4 Loss of anillin induces disorganization of the perijunctional actomyosin belt. DU145 cells transfected with either control or anillin-specific siRNAs were subjected to dual labeling for either **a** filamentous (F) actin (*green*) and β-catenin (*red*) or **b** NM IIB (*green*) and E-cadherin (*red*) on day 4 post-transfection. *Arrows* indicate a well-formed perijunctional actomyosin belt in control cells. *Arrowheads* highlight disorganized perijunctional actin filaments and basal NM IIB-enriched stress fibers in anillin-depleted cells. *Scale bar* 20 μm

pharmacological inhibitor of Rho-associated kinase (ROCK). However, 24 h incubation of control DU145 cells with Y-27632 (25 μM) showed little effect on the integrity of AJ and TJ (Fig. 5d), and assembly of the circumferential F-actin belt (data not shown), despite inhibiting RMLC phosphorylation (Fig. 5e). This result contradicts the potential role of NM II inactivation in the disruption of epithelial junctions following anillin knockdown.

We also investigated whether dysfunctions of CD2AP, Ect2 and MgcRacGAP, which are known anillin-binding partners and important junctional regulators [46–50], are involved in the observed phenomena. Surprisingly, anillin depletion increased expression of all three proteins in DU145 cells (Suppl. Fig. 5a). Furthermore, CD2AP, Ect2, and MgcRacGAP did not associate with epithelial junctions and demonstrated perinuclear or nuclear localization in control DU145 cell monolayers (Suppl. Fig. 5). Together, these results argue against the role of CD2AP, Ect2, and MgcRacGAP in the AJ and TJ disassembly caused by anillin knockdown.

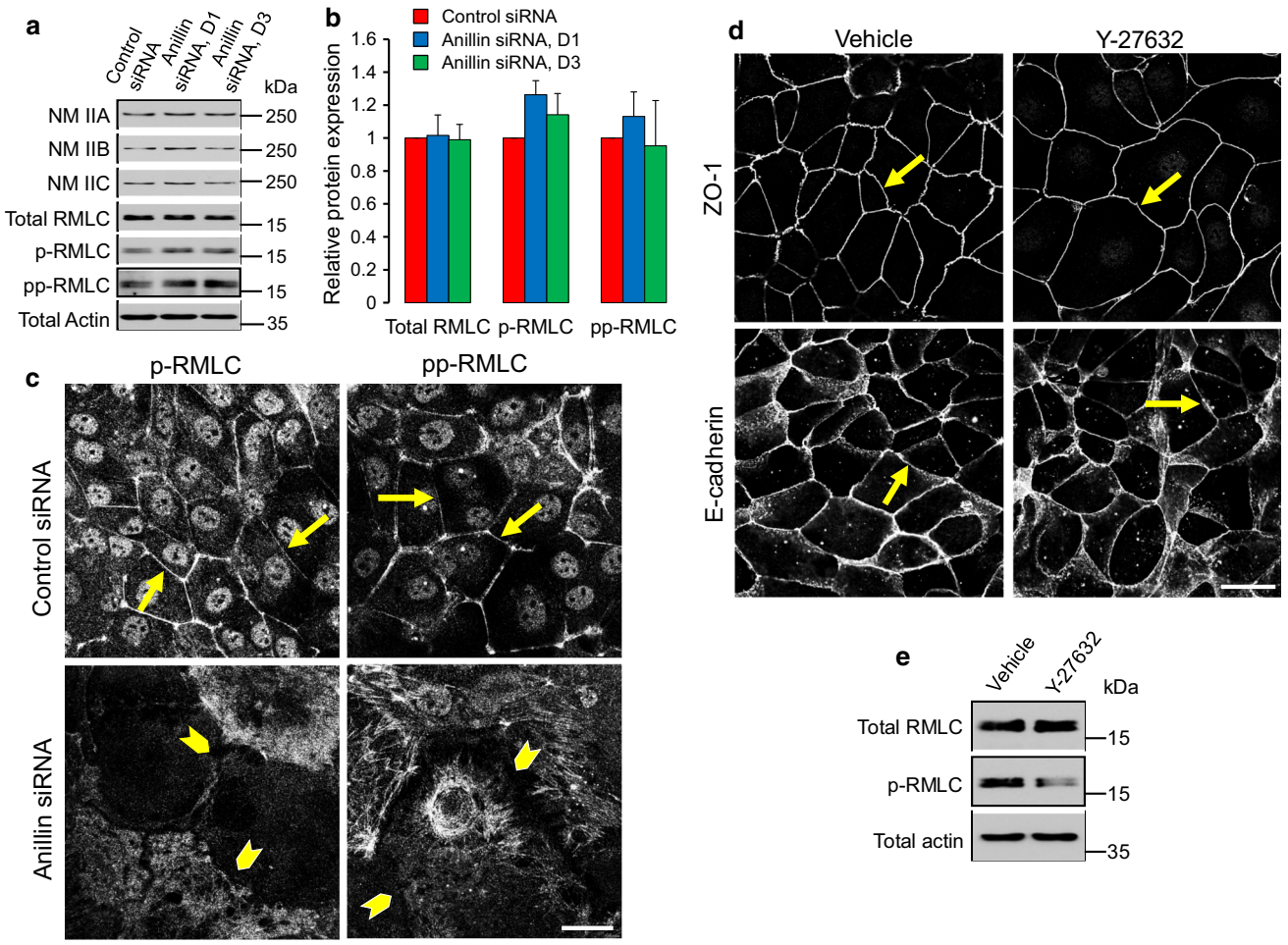

Fig. 5 Effects of anillin depletion on epithelial junctions are not mediated by altered NM II activity. **a**, **b** DU145 cells were transfected with either control or anillin-specific siRNAs (duplex 1 and 3) and were harvested for total cell lysates on day 4 post-transfection. Expression of different NM II heavy chain isoforms, total regulatory myosin light chain (RMLC), as well as monophosphorylated (p) and diphosphorylated (pp) RMLC, was determined by immunoblotting. **c** Control and anillin-depleted DU145 cells were immunolabeled for p-RMLC and pp-RMLC. *Arrows* point out localization of phosphorylated RMLC at epithelial junctions in control DU145 cells, whereas *arrowheads* highlight loss of such localization following anillin depletion. **d**, **e** Control DU145 cells were treated for 24 h with either vehicle, or ROCK inhibitor, Y-27632 (25 μM), and examined for AJ/TJ integrity and RMLC phosphorylation. *Arrows* indicate intact AJ and TJ in either vehicle or Y-27632-treated epithelial cells. *Scale bar* 20 μm

Anillin depletion altered the composition and architecture of the spectrin–adducin membrane skeleton

Out data suggests that loss of anillin selectively affects the cytoskeletal structures associated with areas of cell–cell contact (Figs. 4, 5). A possible mechanism of such spatially restricted cytoskeletal disorganization may involve destabilization of actin filament interactions with the lateral plasma membrane. This idea is indirectly supported by apparently increased protrusiveness of lateral cell–cell contacts in anillin-depleted epithelial cells (Fig. 2), as well as by reported vesiculation of the lateral membranes of anillin null *Drosophila* cells [32]. One of the major mechanisms linking actin filaments to the plasma membrane involves the spectrin–adducin network known as the membrane skeleton [51, 52]. Importantly, adducin and spectrin were previously implicated in remodeling of epithelial junctions [53] and the formation of the lateral plasma membrane domain in polarized epithelial cells [54–56]. Considering this data, we sought to examine the effects of anillin knockdown on the integrity and composition of the membrane skeleton. Immunoblotting analysis revealed dramatic (up to 94 %) downregulation of γ-adducin protein in anillin-depleted DU145 cells (Fig. 6a), and A549 cells (data not shown); whereas, protein levels of neither α-adducin, nor αII- and βII-spectrins were affected. This downregulation of γ-adducin occurred at the transcriptional level, while mRNA expression of α- and β-adducin was elevated (Fig. 6b). Importantly, loss of

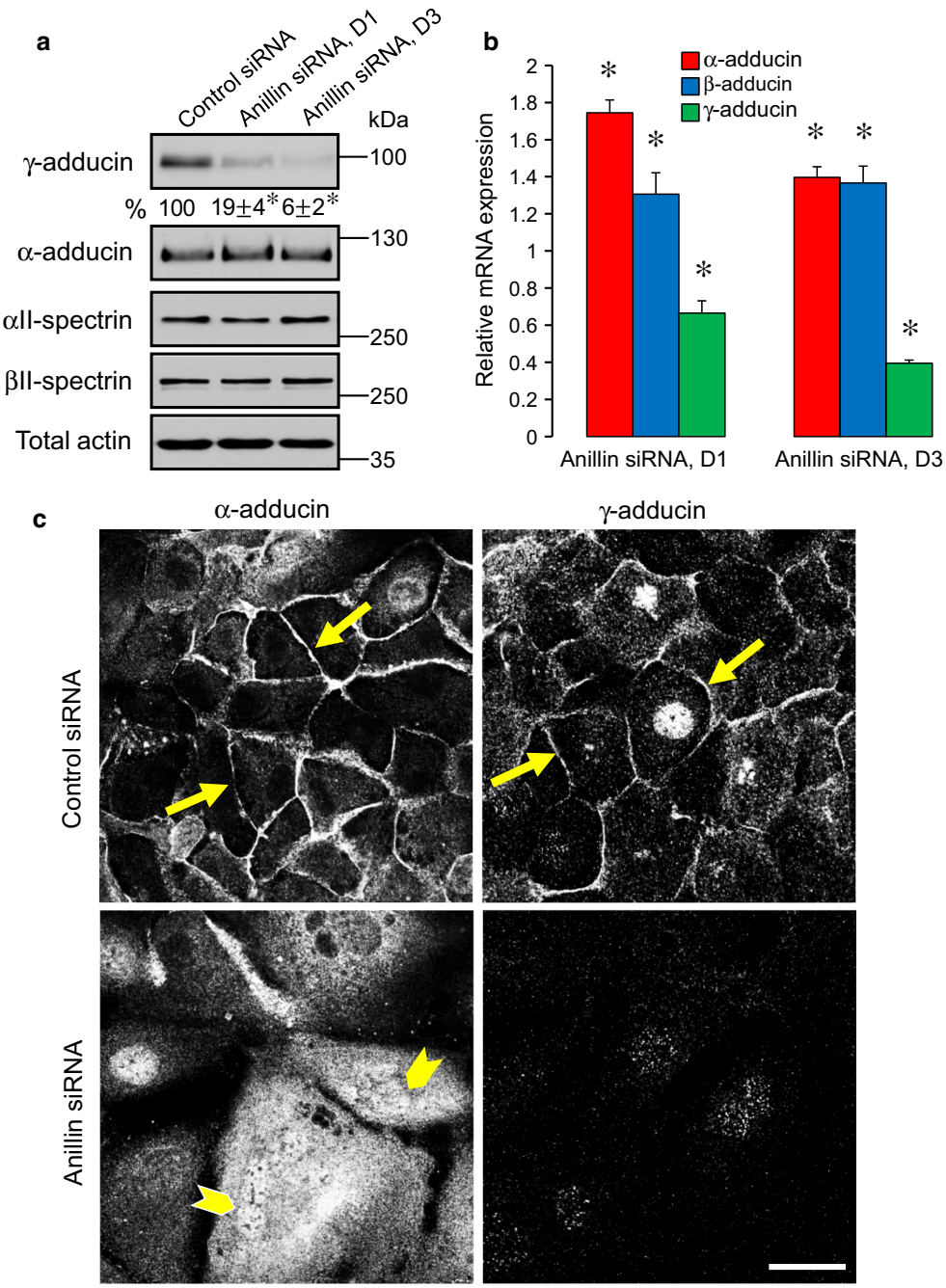

Fig. 6 Anillin depletion alters expression and localization of adducins. Protein (**a**) and mRNA expression (**b**) of adducin and spectrin isoforms was examined in control and anillin-depleted DU145 cells on day 4 post-siRNA transfection. **c** Localization of α-adducin and γ-adducin was determined by immunofluorescence labeling. *Arrows* indicate accumulation of α-adducin and γ-adducin at intercellular junctions in control cells. *Arrowheads* highlight predominantly cytoplasmic labeling of α-adducin after anillin depletion. Data are presented as mean ± SE ($n = 3$); *$p < 0.05$. *Scale bar* 20 μm

anillin induced dramatic reorganization of the lateral membrane skeleton, as manifested by translocation of α-adducin, αII-spectrin, and βII-spectrin from intercellular junctions to the cytoplasm (Figs. 6, 7; Suppl. Fig. 6). The most vivid redistribution was observed for αII-spectrin, which frequently assembled thick cytoplasmic bundles/aggregates positioned in close proximity to intercellular junctions in anillin-depleted cells. Vesicles containing AJ proteins such as β-catenin accumulated behind, or were trapped within, these abnormal αII-spectrin bundles (Fig. 7, arrowheads). Collectively, this data reveals previously unanticipated effects of anillin depletion on the assembly and protein composition of the membrane skeleton associated with epithelial junctions.

In order to elucidate whether loss of γ-adducin contributes to AJ/TJ disassembly in anillin-depleted epithelia, we used RNA interference to downregulate expression of this protein in DU145 cells. Knockdown of γ-adducin efficiently decreased its expression without affecting α-adducin levels (Suppl. Fig. 7). Interestingly, this knockdown recapitulated some effects of anillin deficiency by impairing AJ and TJ integrity, disrupting the perijunctional

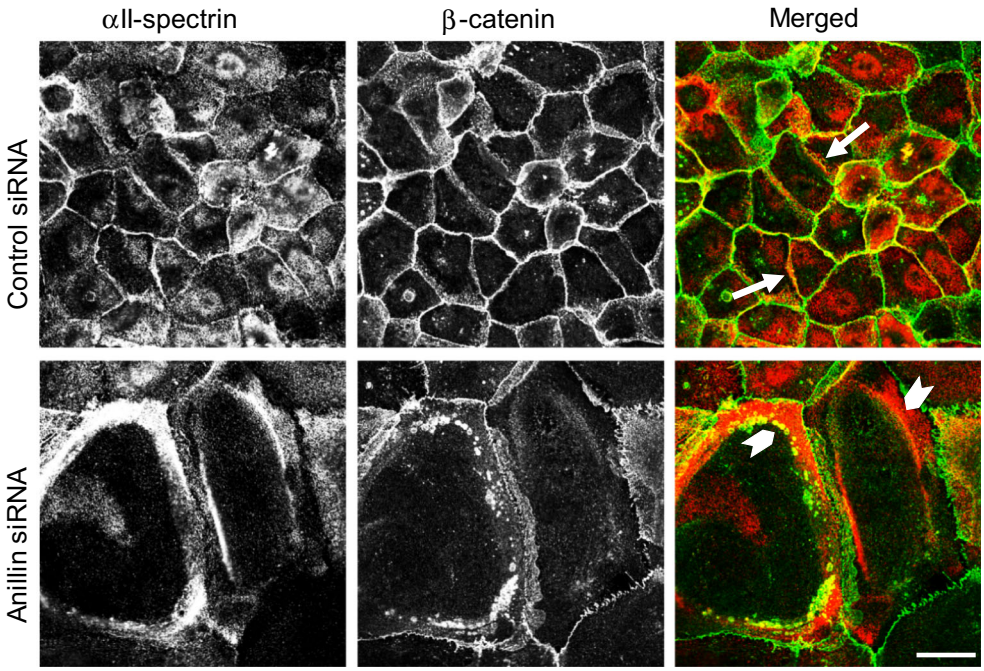

Fig. 7 Anillin depletion affects cellular distribution of α-spectrin. DU145 cells were transfected with either control or anillin-specific siRNAs and subjected to dual immunolabeling for αII-spectrin (*red*) and β-catenin (*green*). *Arrows* indicate localization of αII-spectrin at intercellular junctions in control cells. *Arrowheads* highlight accumulation of cytoplasmic αII-spectrin aggregates in anillin-depleted cells. *Scale bar* 20 μm

F-actin belt (Suppl. Fig. 7c), and reducing junctional accumulation of α-adducin at intercellular contacts (data not shown). However, overexpression of γ-adducin failed to restore junctional integrity in anillin-depleted DU145 cells (Suppl. Fig. 8). This data suggests that loss of γ-adducin does not play a major role in the AJ and TJ disassembly triggered by anillin knockdown.

Activation of c-Jun N-terminal protein kinase mediates junctional disassembly in anillin-depleted epithelial cells

Finally, we sought to elucidate the signaling events that connect nuclear anillin with epithelial junctions. Specifically, we investigated the roles of mitogen-activated protein kinases (MAPK), which are modulated by signaling inputs from different cellular organelles, and are known regulators of epithelial junctions [57–62]. Immunoblotting analysis was used to compare the expression of three major MAPK, namely c-Jun N-terminal protein kinase (JNK), extracellular signal responsive/regulated kinases (ERK) 1/2, and p38 kinase in control and anillin-depleted DU145 cells. Remarkably, the level of phosphorylated (active) JNK was substantially (up to fivefold) increased following anillin knockdown, whereas the activation status of ERK1/2 and p38 was not affected (Fig. 8a). In order to establish a causal role of JNK activation in anillin-dependent junctional disassembly, we used a known pharmacological inhibitor of JNK, SP600125 [63]. Interestingly, 24-h incubation with this inhibitor (25 μM) reversed anillin-dependent AJ and TJ disassembly (Fig. 8b). Moreover, JNK inhibition restored the integrity of the perijunctional actomyosin belt and junctional localization of α-adducin in anillin-depleted cells (Fig. 9). It is of note, AJ and TJ rescue caused by JNK inhibition was not accompanied by restoration of γ-adducin expression (Fig. 8c). This provides another argument against the role of γ-adducin downregulation in junctional defects of anillin-deficient epithelial cells.

Discussion

Anillin is a unique cytoskeletal scaffolding protein that plays essential roles in cell division and embryonic morphogenesis. This protein accumulates in different cellular compartments in a cell cycle-specific fashion; however, its functions in non-dividing cells remain obscure. Our study is the first to identify anillin as an essential regulator of intercellular junctions in human epithelial cell monolayers. We demonstrate that anillin depletion disrupted the normal architecture of AJ and TJ without altering expression of junctional proteins. Such impairment of epithelial junctions was associated with the disassembly of the perijunctional actomyosin belt and loss of the lateral spectrin–adducin membrane skeleton. A recent study described defects in cell–cell adhesions after anillin depletion in *Xenopus* embryos [39]. However, compared to *Xenopus* tissue, our data highlights major differences in the mechanisms of anillin-dependent junctional regulation in mammalian epithelia. For example, in contrast to its *Xenopus* ortholog, we observed that human anillin does not accumulate at intercellular junctions and remains predominantly intra-nuclear in

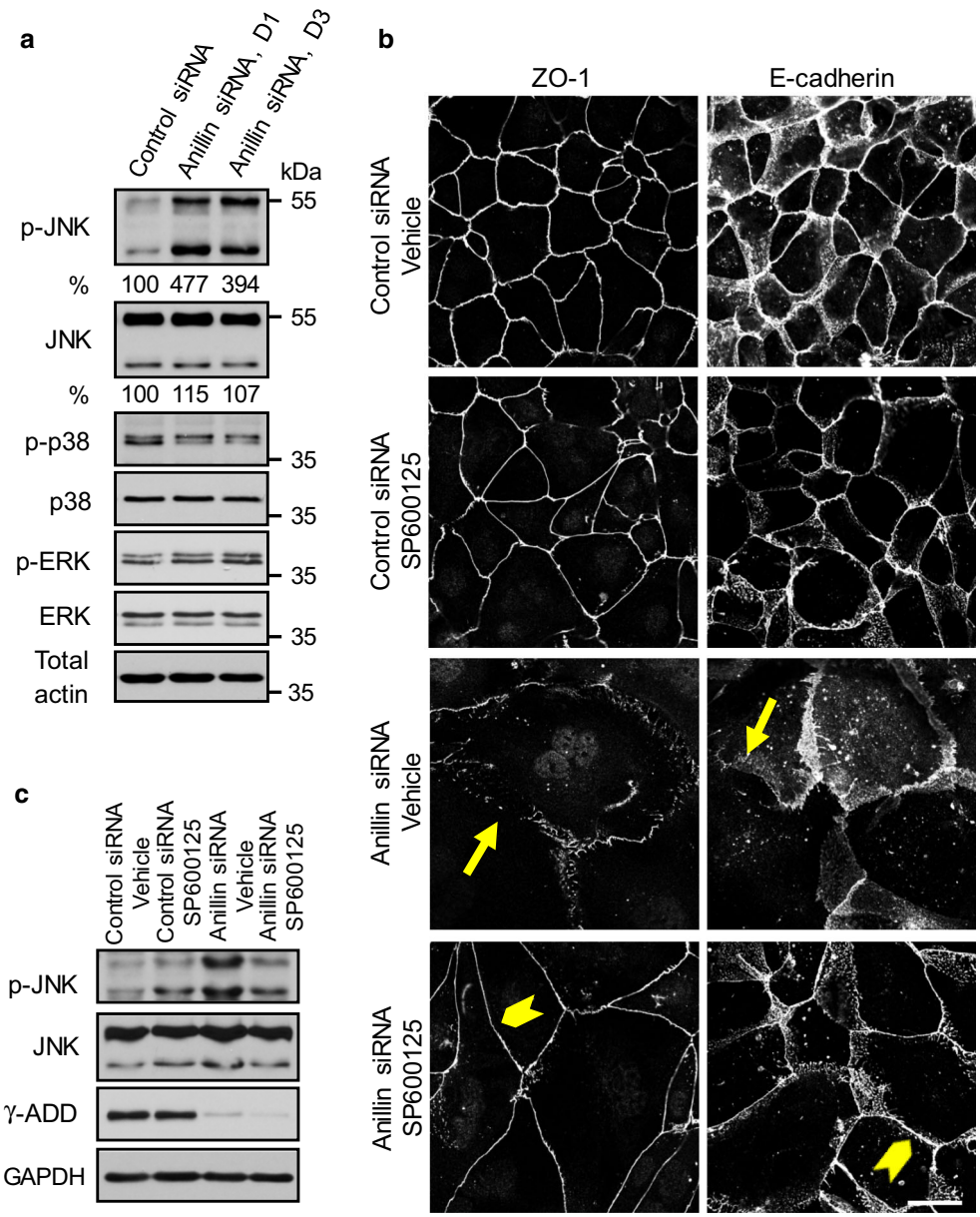

Fig. 8 Activation of JNK mediates junctional disassembly in anillin-depleted epithelial cells. **a** Expression and phosphorylation of three major MAPKs was determined in control and anillin-depleted DU145 cells via immunoblotting. **b**, **c** Control and anillin-depleted DU145 cells were treated for 24 h with either vehicle or JNK inhibitor, SP600125 (25 μM). The effect of JNK inhibition on AJ and TJ integrity was determined by immunolabeling of E-cadherin and ZO-1. JNK activation and expression of γ-adducin was examined by immunoblotting. *Arrows* indicate AJ/TJ disassembly in vehicle-treated anillin-depleted cells. *Arrowheads* highlight restoration of junctional integrity of anillin-depleted cells by JNK inhibition. *Scale bar* 20 μm

interphase DU145, SK-CO15, and A549 cells (Fig. 3, Suppl. Fig. 3, and data not shown). This is consistent with a number of previous studies demonstrating nuclear localization of endogenous anillin in cultured mammalian cells and human tissues [34, 35, 37, 64]. In addition to nuclear localization, diffuse cytoplasmic labeling of anillin was reported in tissue sections of human small intestine, prostate, renal tubules, and salivary gland ducts [64]. A singular example of specific anillin targeting to cell–cell contacts involves its accumulation in the intercalated disc of the human myocardium [64]. This data suggests that in mammals anillin does not play a direct scaffolding role at epithelial AJ and TJ, but instead remotely regulates the integrity of junctional complexes by modulating intracellular signaling cascades.

We found that impaired organization of AJ and TJ in anillin-depleted epithelial cells was accompanied by dramatic rearrangements of the cortical F-actin cytoskeleton. This event included disassembly of the circumferential F-actin belt and loss of junction-associated NM II motor (Fig. 4). Given the large body of evidence implicating the perijunctional actomyosin cytoskeleton in the formation of epithelial AJ and TJ [9, 11, 12, 19], the observed cytoskeletal defects most likely mediate junctional disassembly caused by anillin knockdown. How could anillin regulate cytoskeletal structures associated with epithelial junctions? Integrity of the perijunctional F-actin belt depends on the coordinated activity of NM II motor and the actin-polymerization machinery. Previous studies

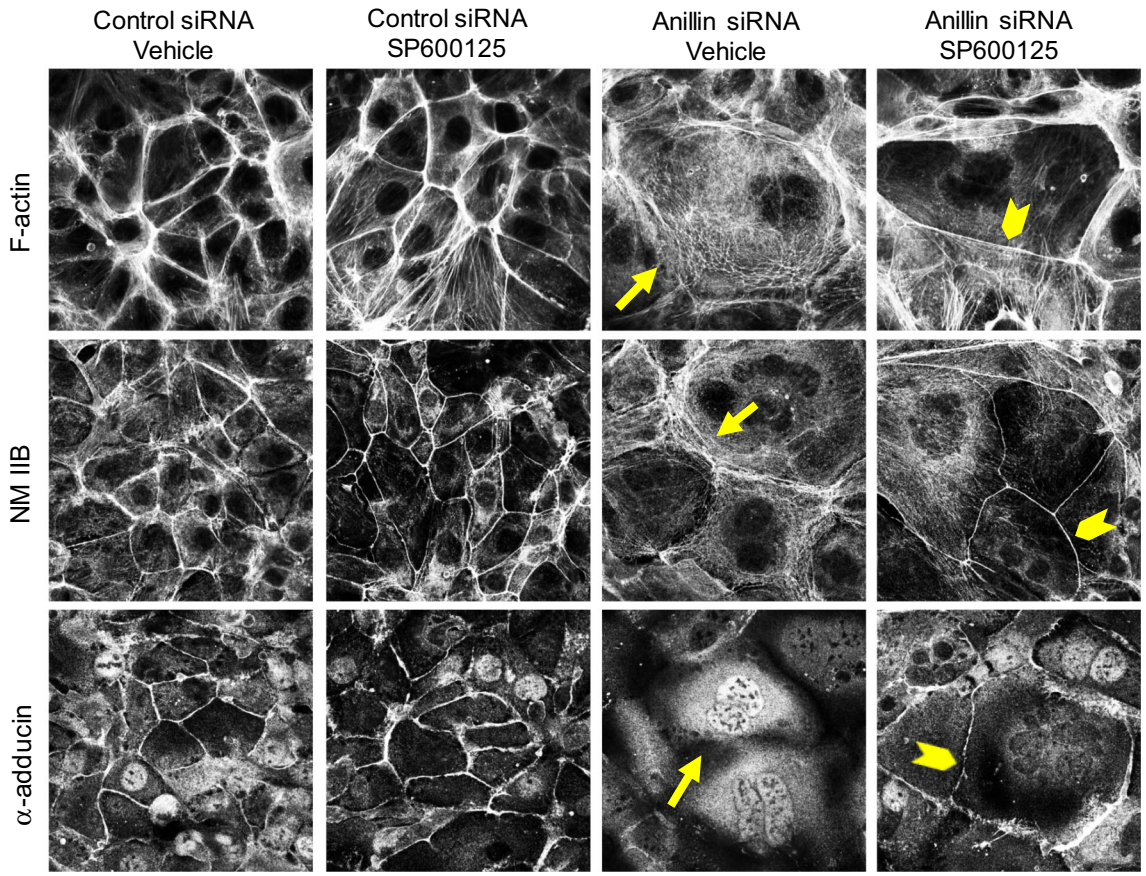

Fig. 9 JNK inhibition restores the perijunctional actomyosin belt and α-adducin localization in anillin-depleted cells. Control and anillin-depleted DU145 cells were treated for 24 h with either vehicle or JNK inhibitor, SP600125 (25 μM). The effect of JNK inhibition on the perijunctional actomyosin cytoskeleton and the membrane skeleton was determined by fluorescence labeling. *Arrows* indicate disruption of F-actin, NM IIB, and α-adducin localization at intercellular contacts of vehicle-treated anillin-depleted cells. *Arrowheads* highlight restoration of the perijunctional actomyosin belt and junction-associated α-adducin fraction in anillin-depleted cells following JNK inhibition. *Scale bar* 20 μm

suggested that anillin could be involved in these two mechanisms. For example, anillin controls localization and activity of Rho GTPase [35, 39], which is a key mediator of RMLC phosphorylation and NM II activity. This effect of anillin is due to its known associations with upstream regulators of Rho activity, such as MgcRacGAP and Ect2 [65–67]. Consistently, manipulation of anillin expression was shown to alter levels of RMLP phosphorylation in human and *Xenopus* epithelia [35, 39]. However, our data conflicts with the notion that inhibition of Rho-ROCK signaling is involved in the impaired cell–cell adhesions of anillin-depleted human epithelial cells. Thus, MgcRacGAP and Ect2 did not localize at epithelial junctions in control DU145 cell monolayers, and were not depleted, but rather overexpressed following anillin knockdown (Suppl. Fig. 5). Furthermore, anillin depletion did not affect NM II activation, as indicated by the unaltered cellular level of phosphorylated RMLC (Fig. 5a, b). Finally, blocking RMLC phosphorylation with ROCK inhibitor was not sufficient to trigger AJ/TJ disassembly in control DU145 cells (Fig. 5d). An alternative mechanism of anillin-dependent regulation of the perijunctional actin cytoskeleton may involve modulation of actin filament turnover. This concept involves established anillin interactions with the F-actin capping protein, CD2AP [37], which was previously implicated in the regulation of AJ and TJ integrity [46, 50, 68]. However, in our experimental system, CD2AP was neither enriched at normal epithelial junctions, nor downregulated by anillin knockdown (Suppl. Fig. 5). Hence, CD2AP is unlikely to be responsible for disintegration of the perijunctional cytoskeletal observed in anillin-depleted epithelial cells.

It is important to note that loss of anillin did not cause global cytoskeletal defects, such as general loss or disorganization of F-actin bundles. Instead, it selectively disrupted the integrity of the perijunctional actomyosin belt (Fig. 4). The most plausible explanation for such a selective effect is that anillin depletion disrupted organization of

the spectrin–adducin membrane skeleton, which is essential for correct localization and assembly of F-actin bundles at the lateral plasma membrane and intercellular junctions. Spectrin forms an elaborate polymeric network at the cytoplasmic face of the plasma membrane [51, 52]. This network enhances the lateral membrane in epithelial cells, guides assembly of cortical actin filaments, and strengthens intercellular adhesions [69, 70]. Spectrin association with actin filaments is greatly accelerated by adducin proteins, which could also regulate F-actin in a spectrin-independent fashion, due to their intrinsic F-actin bundling and capping activity [52, 71]. We observed severe disruption of the spectrin–adducin network associated with epithelial junctions in anillin-depleted epithelial cells. This disruption involved selective downregulation of γ-adducin expression, translocation of α-adducin and spectrins from the plasma membrane into cytoplasmic/nuclear compartments, and formation of abnormal cytoplasmic αII-spectrin filaments (Figs. 6, 7; Suppl. Fig. 6). To our knowledge, this is the first evidence that implicates anillin in the regulation of the spectrin–adducin membrane skeleton. The decrease in γ-adducin protein and mRNA levels following anillin knockdown (Fig. 6) is particularly intriguing since anillin has not been previously linked to the regulation of protein expression. Mechanisms of such regulation remain unknown although the nuclear localization and actin-binding ability of anillin suggest that it may modulate the activity of actin-dependent transcriptional machinery [72, 73].

Several recent studies demonstrated essential roles of adducin and spectrins in the assembly of the perijunctional actin cytoskeleton and AJ/TJ integrity in different experimental systems [53, 54, 56, 74–76]. Consequently, the observed disruption of the spectrin–adducin network is likely to be involved in junctional disassembly following anillin depletion. Although γ-adducin knockdown recapitulated some effects of anillin depletion by impairing the integrity of epithelial junctions and organization of the perijunctional cytoskeleton (Suppl. Fig. 7), downregulation of γ-adducin alone cannot account for the AJ/TJ disassembly caused by anillin deficiency (Suppl. Fig. 8). This likely reflects a cross-talk between several mechanisms involving different elements of the membrane skeleton and the actin cytoskeleton. The abnormal aggregation of α-spectrin could be particularly important because it creates a physical barrier interrupting trafficking of junctional proteins to the areas of cell–cell contact (Fig. 7).

The present study identified a key signaling mechanism that mediates disassembly of epithelial junctions triggered by anillin depletion. This mechanism involves selective activation of JNK (Fig. 8) that appears to be responsible for the observed disorganization of the perijunctional actin cytoskeleton and the membrane skeleton, as well as for the disruption of AJ and TJ (Fig. 9). Importantly, JNK inhibition specifically restored the integrity of epithelial junctions without rescuing other morphological alterations, such as enlargements and multinucleation of anillin-depleted epithelial cells (Figs. 8, 9, and data not shown). This strongly suggests that AJ and TJ disassembly represents a specific consequence of anillin depletion, which is independent of defective cytokinesis. Our findings fittingly agree with the emerging role of JNK in the regulation of epithelial junctions [58, 62]. Thus, many environmental stimuli are known to disrupt AJ and TJ integrity via JNK activation, whereas inhibition of JNK signaling promotes junctional assembly and enhances epithelial barriers in vitro and in vivo [59, 77–80]. JNK activation disrupts epithelial junctions via multiple mechanisms. These mechanisms include direct phosphorylation of β-catenin, impairing protein interactions at AJ [78, 79], as well as altered expression of TJ proteins [81, 82]. Moreover, JNK reportedly regulates actin cytoskeleton dynamics and organization of the membrane skeleton. The former effect has been linked to JNK-dependent modulation of different actin-binding proteins, such as ezrin, drebrin, and filamin in epithelial cells [59, 77, 83]. The latter effect was manifested by JNK-dependent phosphorylation of adducins in tumor cells [84], and disorganization of cortical α-spectrin in cardiomyocytes [85]. While our data strongly supports the role of JNK activation in AJ/TJ disassembly caused by anillin depletion, two key questions remain unanswered. One question is which molecular targets of activated JNK can mediate cytoskeletal reorganization and junctional disruption, while the other question is about the mechanisms of anillin-dependent regulation of JNK activity. Although anillin is known to interact with several signaling molecules including protein phosphatase 2A, citron kinase, CIN85 kinase adaptor, etc. [86], there is no published data regarding its interactions with JNK or upstream regulators of the JNK signaling cascade. Future studies are warranted to answer these important questions. In conclusion, our study provides compelling evidence that anillin serves as an essential regulator of human epithelial barriers, which modulates JNK signaling to maintain the assembly of apical junctions, and proper organization of the perijunctional F-actin cytoskeleton and the cortical membrane skeleton.

Acknowledgments We thank Drs. Charles A. Parkos, Y. Peng Loh, Enrique Rodriguez-Boulan, and Andrei Budanov for providing reagents for this study. Microscopy was performed at the VCU Department of Anatomy and Neurobiology Microscopy Facility, supported, in part, with funding from the NIH-NINDS Center core grant 5P30NS047463. This work was supported by National Institute of Health grants RO1 DK083968 and DK084953 to A.I.I.

Conflict of interests The authors declared no conflict of interests.

References

1. Anderson JM, Van Itallie CM (2009) Physiology and function of the tight junction. Cold Spring Harb Perspect Biol 1:a002584
2. Cheng CY, Mruk DD (2012) The blood-testis barrier and its implications for male contraception. Pharmacol Rev 64:16–64
3. Turner JR (2009) Intestinal mucosal barrier function in health and disease. Nat Rev Immunol 9:799–809
4. Green KJ, Getsios S, Troyanovsky S, Godsel L (2010) Intercellular junction assembly, dynamics, and homeostasis. Cold Spring Harb Perspect Biol 2:a000125
5. Tsukita S, Furuse M, Itoh M (2001) Multifunctional strands in tight junctions. Nat Rev Mol Cell Biol 2:285–293
6. Furuse M (2010) Molecular basis of the core structure of tight junctions. Cold Spring Harb Perspect Biol 2:a002907
7. Furuse M, Izumi Y, Oda Y, Higashi T, Iwamoto N (2014) Molecular organization of tricellular tight junctions. Tissue barriers 2:e28960
8. Meng W, Takeichi M (2009) Adherens junction: molecular architecture and regulation. Cold Spring Harb Perspect Biol 1:a002899
9. Troyanovsky S (2012) Adherens junction assembly. Subcell Biochem 60:89–108
10. Van Itallie CM, Anderson JM (2013) Claudin interactions in and out of the tight junction. Tissue barriers 1:e25247
11. Han SP, Yap AS (2012) The cytoskeleton and classical cadherin adhesions. Subcell Biochem 60:111–135
12. Ivanov AI (2008) Actin motors that drive formation and disassembly of epithelial apical junctions. Front Biosci 13:6662–6681
13. Ivanov AI, Naydenov NG (2013) Dynamics and regulation of epithelial adherens junctions: recent discoveries and controversies. Int Rev Cell Mol Biol 303:27–99
14. Shen L, Weber CR, Raleigh DR, Yu D, Turner JR (2011) Tight junction pore and leak pathways: a dynamic duo. Annu Rev Physiol 73:283–309
15. Troyanovsky SM (2008) Regulation of cadherin-based epithelial cell adhesion by endocytosis. Front Biosci Scholar Ed 1:61–67
16. Hirokawa N, Heuser JE (1981) Quick-freeze, deep-etch visualization of the cytoskeleton beneath surface differentiations of intestinal epithelial cells. J Cell Biol 91:399–409
17. Hirokawa N, Tilney LG (1982) Interactions between actin filaments and between actin filaments and membranes in quick-frozen and deeply etched hair cells of the chick ear. J Cell Biol 95:249–261
18. Madara JL (1987) Intestinal absorptive cell tight junctions are linked to cytoskeleton. Am J Physiol 253:C171–C175
19. Ivanov AI, Parkos CA, Nusrat A (2010) Cytoskeletal regulation of epithelial barrier function during inflammation. Am J Pathol 177:512–524
20. Yonemura S (2011) Cadherin–actin interactions at adherens junctions. Curr Opin Cell Biol 23:515–522
21. Takeichi M (2014) Dynamic contacts: rearranging adherens junctions to drive epithelial remodelling. Nat Rev Mol Cell Biol 15:397–410
22. Dominguez R, Holmes KC (2011) Actin structure and function. Annu Rev Biophys 40:169
23. Dos Remedios C, Chhabra D, Kekic M, Dedova I, Tsubakihara M, Berry D, Nosworthy N (2003) Actin binding proteins: regulation of cytoskeletal microfilaments. Physiol Rev 83:433–473
24. Citalán-Madrid AF, García-Ponce A, Vargas-Robles H, Betanzos A, Schnoor M (2013) Small GTPases of the Ras superfamily regulate intestinal epithelial homeostasis and barrier function via common and unique mechanisms. Tissue barriers 1:e26938
25. McCole DF (2013) Phosphatase regulation of intercellular junctions. Tissue barriers 1:e26713
26. Vicente-Manzanares M, Ma X, Adelstein RS, Horwitz AR (2009) Non-muscle myosin II takes centre stage in cell adhesion and migration. Nat Rev Mol Cell Biol 10:778–790
27. D'Avino PP (2009) How to scaffold the contractile ring for a safe cytokinesis–lessons from Anillin-related proteins. J Cell Sci 122:1071–1079
28. Hickson GR, O'Farrell PH (2008) Anillin: a pivotal organizer of the cytokinetic machinery. Biochem Soc Trans 36:439
29. Piekny AJ, Maddox AS (2010) The myriad roles of Anillin during cytokinesis. Semin Cell Dev Biol 21:881–891
30. Field CM, Alberts BM (1995) Anillin, a contractile ring protein that cycles from the nucleus to the cell cortex. J Cell Biol 131:165–178
31. Kinoshita M, Field CM, Coughlin ML, Straight AF, Mitchison TJ (2002) Self-and actin-templated assembly of mammalian septins. Dev Cell 3:791–802
32. Field CM, Coughlin M, Doberstein S, Marty T, Sullivan W (2005) Characterization of anillin mutants reveals essential roles in septin localization and plasma membrane integrity. Development 132:2849–2860
33. Piekny AJ, Glotzer M (2008) Anillin is a scaffold protein that links RhoA, actin, and myosin during cytokinesis. Curr Biol 18:30–36
34. Straight AF, Field CM, Mitchison TJ (2005) Anillin binds nonmuscle myosin II and regulates the contractile ring. Mol Biol Cell 16:193–201
35. Suzuki C, Daigo Y, Ishikawa N, Kato T, Hayama S, Ito T, Tsuchiya E, Nakamura Y (2005) ANLN plays a critical role in human lung carcinogenesis through the activation of RHOA and by involvement in the phosphoinositide 3-kinase/AKT pathway. Cancer Res 65:11314–11325
36. Dorn JF, Zhang L, Paradis V, Edoh-Bedi D, Jusu S, Maddox PS, Maddox AS (2010) Actomyosin tube formation in polar body cytokinesis requires anillin in *C. elegans*. Curr Biol 20:2046–2051
37. Gbadegesin RA, Hall G, Adeyemo A, Hanke N, Tossidou I, Burchette J, Wu G, Homstad A, Sparks MA, Gomez J, Jiang R, Alonso A, Lavin P, Conlon P, Korstanje R, Stander MC, Shamsan G, Barua M, Spurney R, Singhal PC, Kopp JB, Haller H, Howell D, Pollak MR, Shaw AS, Schiffer M, Winn MP (2014) Mutations in the gene that encodes the F-actin binding protein anillin cause FSGS. J Am Soc Nephrol 25:1991–2002
38. Toret CP, D'Ambrosio MV, Vale RD, Simon MA, Nelson WJ (2014) A genome-wide screen identifies conserved protein hubs required for cadherin-mediated cell–cell adhesion. J Cell Biol 204:265–279
39. Reyes CC, Jin M, Breznau EB, Espino R, Delgado-Gonzalo R, Goryachev AB, Miller AL (2014) Anillin regulates cell-cell junction integrity by organizing junctional accumulation of Rho-GTP and actomyosin. Curr Biol 24:1263–1270
40. Liu Y, Nusrat A, Schnell FJ, Reaves TA, Walsh S, Pochet M, Parkos CA (2000) Human junction adhesion molecule regulates tight junction resealing in epithelia. J Cell Sci 113(Pt 13):2363–2374
41. Baranwal S, Naydenov NG, Harris G, Dugina V, Morgan KG, Chaponnier C, Ivanov AI (2012) Nonredundant roles of cytoplasmic beta- and gamma-actin isoforms in regulation of epithelial apical junctions. Mol Biol Cell 23:3542–3553
42. Naydenov NG, Baranwal S, Khan S, Feygin A, Gupta P, Ivanov AI (2013) Novel mechanism of cytokine-induced disruption of epithelial barriers: janus kinase and protein kinase D-dependent downregulation of junction protein expression. Tissue Barriers 1:e25231

43. Lou H, Park JJ, Phillips A, Loh YP (2013) gamma-Adducin promotes process outgrowth and secretory protein exit from the Golgi apparatus. J Mol Neurosci 49:1–10
44. Chen HC (2005) Cell-scatter assay. Methods Mol Biol 294:69–77
45. Echard A, Hickson GR, Foley E, O'Farrell PH (2004) Terminal cytokinesis events uncovered after an RNAi screen. Curr Biol 14:1685–1693
46. Elbediwy A, Zihni C, Terry SJ, Clark P, Matter K, Balda MS (2012) Epithelial junction formation requires confinement of Cdc42 activity by a novel SH3BP1 complex. J Cell Biol 198:677–693
47. Guillemot L, Guerrera D, Spadaro D, Tapia R, Jond L, Citi S (2014) MgcRacGAP interacts with cingulin and paracingulin to regulate Rac1 activation and development of the tight junction barrier during epithelial junction assembly. Mol Biol Cell 25:1995–2005
48. Priya R, Yap AS, Gomez GA (2013) E-cadherin supports steady-state Rho signaling at the epithelial zonula adherens. Differentiation 86:133–140
49. Ratheesh A, Gomez GA, Priya R, Verma S, Kovacs EM, Jiang K, Brown NH, Akhmanova A, Stehbens SJ, Yap AS (2012) Centralspindlin and alpha-catenin regulate Rho signalling at the epithelial zonula adherens. Nat Cell Biol 14:818–828
50. Tang VW, Brieher WM (2013) FSGS3/CD2AP is a barbed-end capping protein that stabilizes actin and strengthens adherens junctions. J Cell Biol 203:815–833
51. Bennett V, Baines AJ (2001) Spectrin and ankyrin-based pathways: metazoan inventions for integrating cells into tissues. Physiol Rev 81:1353–1392
52. Fowler VM (2012) The human erythrocyte plasma membrane: a rosetta stone for decoding membrane-cytoskeleton structure. Curr Top Membr 72:39–88
53. Naydenov NG, Ivanov AI (2010) Adducins regulate remodeling of apical junctions in human epithelial cells. Mol Biol Cell 21:3506–3517
54. Abdi KM, Bennett V (2008) Adducin promotes micrometer-scale organization of β2-spectrin in lateral membranes of bronchial epithelial cells. Mol Biol Cell 19:536–545
55. Kizhatil K, Davis JQ, Davis L, Hoffman J, Hogan BL, Bennett V (2007) Ankyrin-G is a molecular partner of E-cadherin in epithelial cells and early embryos. J Biol Chem 282:26552–26561
56. Kizhatil K, Yoon W, Mohler PJ, Davis LH, Hoffman JA, Bennett V (2007) Ankyrin-G and β2-spectrin collaborate in biogenesis of lateral membrane of human bronchial epithelial cells. J Biol Chem 282:2029–2037
57. Kevil CG, Oshima T, Alexander JS (2001) The role of p38 MAP kinase in hydrogen peroxide mediated endothelial solute permeability. Endothelium 8:107–116
58. Kojima T, Yamaguchi H, Ito T, Kyuno D, Kono T, Konno T, Sawada N (2013) Tight junctions in human pancreatic duct epithelial cells. Tissue barriers 1:e24894
59. Naydenov NG, Hopkins AM, Ivanov AI (2009) c-Jun N-terminal kinase mediates disassembly of apical junctions in model intestinal epithelia. Cell Cycle 8:2110–2121
60. Samak G, Aggarwal S, Rao RK (2011) ERK is involved in EGF-mediated protection of tight junctions, but not adherens junctions, in acetaldehyde-treated Caco-2 cell monolayers. Am J Physiol Gastrointest Liver Physiol 301:G50–G59
61. Spindler V, Rotzer V, Dehner C, Kempf B, Gliem M, Radeva M, Hartlieb E, Harms GS, Schmidt E, Waschke J (2013) Peptide-mediated desmoglein 3 crosslinking prevents pemphigus vulgaris autoantibody-induced skin blistering. J Clin Invest 123:800–811
62. You H, Lei P, Andreadis ST (2013) JNK is a novel regulator of intercellular adhesion. Tissue Barriers 1:e26845
63. Bennett BL, Sasaki DT, Murray BW, O'Leary EC, Sakata ST, Xu W, Leisten JC, Motiwala A, Pierce S, Satoh Y, Bhagwat SS, Manning AM, Anderson DW (2001) SP600125, an anthrapyrazolone inhibitor of Jun N-terminal kinase. Proc Natl Acad Sci U S A 98:13681–13686
64. Hall PA, Todd CB, Hyland PL, McDade SS, Grabsch H, Hillan KJ, Russell SH (2005) The septin-binding protein anillin is overexpressed in diverse human tumors. Clin Cancer Res 11:6780–6786
65. D'Avino PP, Takeda T, Capalbo L, Zhang W, Lilley KS, Laue ED, Glover DM (2008) Interaction between Anillin and RacGAP50C connects the actomyosin contractile ring with spindle microtubules at the cell division site. J Cell Sci 121:1151–1158
66. Frenette P, Haines E, Loloyan M, Kinal M, Pakarian P, Piekny A (2012) An anillin-Ect2 complex stabilizes central spindle microtubules at the cortex during cytokinesis. PLoS One 7:e34888
67. Gregory SL, Ebrahimi S, Milverton J, Jones WM, Bejsovec A, Saint R (2008) Cell division requires a direct link between microtubule-bound RacGAP and Anillin in the contractile ring. Curr Biol 18:25–29
68. Xia W, Mruk DD, Lee WM, Cheng CY (2006) Differential interactions between transforming growth factor-beta3/TbetaR1, TAB 1, and CD2AP disrupt blood-testis barrier and Sertoli-germ cell adhesion. J Biol Chem 281:16799–16813
69. Bennett V, Healy J (2009) Membrane domains based on ankyrin and spectrin associated with cell–cell interactions. Cold Spring Harb Perspect Biol 1:a003012
70. Naydenov NG, Ivanov AI (2011) Spectrin-adducin membrane skeleton: a missing link between epithelial junctions and the actin cytoskeletion? Bioarchitecture 1:186–191
71. Matsuoka Y, Li X, Bennett V (2000) Adducin: structure, function and regulation. Cell Mol Life Sci 57:884–895
72. Olson EN, Nordheim A (2010) Linking actin dynamics and gene transcription to drive cellular motile functions. Nat Rev Mol Cell Biol 11:353–365
73. Zheng B, Han M, Bernier M, Wen JK (2009) Nuclear actin and actin-binding proteins in the regulation of transcription and gene expression. FEBS J 276:2669–2685
74. Chen CL, Lin YP, Lai YC, Chen HC (2011) α-Adducin translocates to the nucleus upon loss of cell–cell adhesions. Traffic 12:1327–1340
75. Miyauchi JT, Piermarini PM, Yang JD, Gilligan DM, Beyenbach KW (2013) Roles of PKC and phospho-adducin in transepithelial fluid secretion by Malpighian tubules of the yellow fever mosquito. Tissue Barriers 1:e23120
76. Rötzer V, Breit A, Waschke J, Spindler V (2014) Adducin is required for desmosomal cohesion in keratinocytes. J Biol Chem 289:14925–14940
77. Konno T, Ninomiya T, Kohno T, Kikuchi S, Sawada N, Kojima T (2014) c-Jun N-terminal kinase inhibitor SP600125 enhances barrier function and elongation of human pancreatic cancer cell line HPAC in a Ca-switch model. Histochem Cell Biol 16:16
78. Lee MH, Koria P, Qu J, Andreadis ST (2009) JNK phosphorylates beta-catenin and regulates adherens junctions. FASEB J 23:3874–3883
79. Lee MH, Padmashali R, Koria P, Andreadis ST (2011) JNK regulates binding of alpha-catenin to adherens junctions and cell-cell adhesion. FASEB J 25:613–623
80. Samak G, Chaudhry KK, Gangwar R, Narayanan D, Jaggar JH, Rao R (2015) Calcium/Ask1/MKK7/JNK2/c-Src signalling cascade mediates disruption of intestinal epithelial tight junctions by dextran sulfate sodium. Biochem J 465:503–515
81. Al-Sadi R, Ye D, Boivin M, Guo S, Hashimi M, Ereifej L, Ma TY (2014) Interleukin-6 modulation of intestinal epithelial tight junction permeability is mediated by JNK pathway activation of claudin-2 gene. PLoS One 9:e85345
82. Carrozzino F, Pugnale P, Feraille E, Montesano R (2009) Inhibition of basal p38 or JNK activity enhances epithelial barrier

function through differential modulation of claudin expression. Am J Physiol Cell Physiol 297:C775–C787
83. Kulshammer E, Uhlirova M (2013) The actin cross-linker Filamin/Cheerio mediates tumor malignancy downstream of JNK signaling. J Cell Sci 126:927–938
84. Ma PC, Tretiakova MS, Nallasura V, Jagadeeswaran R, Husain AN, Salgia R (2007) Downstream signalling and specific inhibition of c-MET/HGF pathway in small cell lung cancer: implications for tumour invasion. Br J Cancer 97:368–377
85. Ursitti JA, Petrich BG, Lee PC, Resneck WG, Ye X, Yang J, Randall WR, Bloch RJ, Wang Y (2007) Role of an alternatively spliced form of alphaII-spectrin in localization of connexin 43 in cardiomyocytes and regulation by stress-activated protein kinase. J Mol Cell Cardiol 42:572–581
86. Smith TC, Fridy PC, Li Y, Basil S, Arjun S, Friesen RM, Leszyk J, Chait BT, Rout MP, Luna EJ (2013) Supervillin binding to myosin II and synergism with anillin are required for cytokinesis. Mol Biol Cell 24:3603–3619